

# UC Berkeley

## UC Berkeley Previously Published Works

### Title

A singular flexible cathode for room temperature sodium/sulfur battery

### Permalink

<https://escholarship.org/uc/item/4w42b6r9>

### Authors

Kim, Icpyo  
Kim, Chang Hyeon  
Choi, Sun hwa  
et al.

### Publication Date

2016-03-01

### DOI

10.1016/j.jpowsour.2015.12.035

Peer reviewed



## A singular flexible cathode for room temperature sodium/sulfur battery



Icpyo Kim <sup>a</sup>, Chang Hyeon Kim <sup>b</sup>, Sun hwa Choi <sup>b</sup>, Jae-Pyoung Ahn <sup>c</sup>, Jou-Hyeon Ahn <sup>d</sup>,  
Ki-Won Kim <sup>a, b</sup>, Elton J. Cairns <sup>e, f</sup>, Hyo-Jun Ahn <sup>a, b, \*</sup>

<sup>a</sup> School of Materials Science and Engineering, RIGET, Gyeongsang National University, Jinju, 660-701, South Korea

<sup>b</sup> Department of Materials Engineering and Convergence Technology, Gyeongsang National University, Jinju, 660-701, South Korea

<sup>c</sup> Advanced Analysis Center, Research Planning & Coordination Division, KIST, Seoul, 136-791, South Korea

<sup>d</sup> Department of Chemical & Biological Engineering, Gyeongsang National University, Jinju, 660-701, South Korea

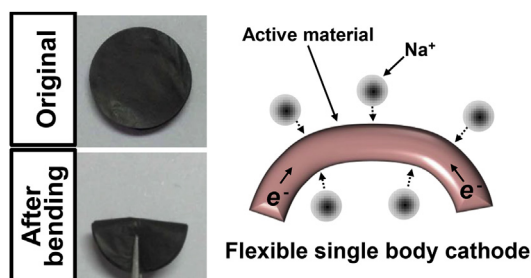
<sup>e</sup> Lawrence Berkeley National Laboratory, Environmental Energy Technologies Division, Berkeley, United States

<sup>f</sup> Department of Chemical and Biomolecular Engineering, University of California, Berkeley, CA 94720, United States

### HIGHLIGHTS

- A flexible sulfurized polyacrylonitrile cathode was prepared by simple pyrolysis.
- The SPAN cathode shows rollability, and bendability to 180° without fracture.
- The cathode contains no binder, current collector and conducting additives.
- Na/SPAN cell shows good cycle performance.
- The 1st capacity of 342 mAh g<sup>-1</sup> electrode remains 266 mAh g<sup>-1</sup> after 200 cycles.

### GRAPHICAL ABSTRACT



### ARTICLE INFO

#### Article history:

Received 14 October 2015

Received in revised form

18 November 2015

Accepted 10 December 2015

Available online xxx

#### Keywords:

Electrospinning

Sulfurized polyacrylonitrile

Nanofiber web

Flexible electrode

Sulfur cathode

Sodium/sulfur battery

### ABSTRACT

This study introduces a new flexible cathode that contains no binder, conductive additive and current collector, but instead consists solely of a sulfurized polyacrylonitrile nanofiber (SPAN) web which is prepared by a simple pyrolysis process with low cost raw materials. This not only exhibits good electrochemical properties, but also a high flexibility, rollability, and bendability to 180° without fracture. Its feasibility as a cathode for a low cost and flexible Na/S battery is subsequently evaluated on the basis that S, PAN, and Na are cheap materials. The SPAN web delivers a high first discharge capacity of 604 mAh g<sup>-1</sup> – electrode (1473 mAh g<sup>-1</sup> – sulfur) at 0.01 C based on sulfur content. In cycle performance at 0.1 C, a first discharge capacity of 342 mAh g<sup>-1</sup> – electrode is obtained and remains over 266 mAh g<sup>-1</sup> – electrode after 200 cycles along with the coulombic efficiency near 100% from the second cycle. In terms of rate capability, it is shown to be capable of delivering a capacity of as high as 71 mAh g<sup>-1</sup> at 1 C. The reversible electrochemical reaction of the SPAN web with Na is related to a reversible bond between the C–S and S–S bonds of the SPAN web.

© 2015 Elsevier B.V. All rights reserved.

\* Corresponding author.

E-mail address: [ahj@gnu.ac.kr](mailto:ahj@gnu.ac.kr) (H.-J. Ahn).

## 1. Introduction

We currently live in a world where portable electronic devices such as cellular phones and laptop computers are much thinner and lighter than the heavy, thick, rigid, and bulky designs of the past. The future development of such devices will be therefore toward even more portable, ultrathin/lightweight, and flexible devices. Products from the developments may include roll-up displays, conformable active RFID tags, e-skins, wearable sensors, and implantable medical devices [1–7].

As such products have typically obtained their electric power from lithium ion batteries, the same goals also apply to battery technology. Consequently, there have been a number of studies aimed at developing flexible electrodes for lithium ion cells [8].

However the very limited resources of lithium (typically in the order of 20 mg kg<sup>-1</sup> in the earth's crust and 0.18 mg L<sup>-1</sup> in seawater) has created a high price for the metal that is expected to only increase in the future. In contrast, sodium is abundant and cheap, with concentrations as high as 28,400 mg kg<sup>-1</sup> earth's crust and 11,000 mg L<sup>-1</sup> in seawater. And sulfur as the cathode active material has many advantages such as high theoretical capacity of 1672 mAh g<sup>-1</sup>, and abundance (340 mg kg<sup>-1</sup> earth's crust). The overall electrochemical reaction of the room temperature Na/S battery is  $2\text{Na} + \text{S} \rightarrow \text{Na}_2\text{S}$ , along with the high theoretical energy density of 1230 W h kg<sup>-1</sup>. After the first report in 2006 [9], a number of studies has been reported [10–17]. And they has pointed out overcoming the low electric conductivity of elemental sulfur and the dissolution of the high order sodium polysulfides causing the various drawbacks such as fast capacity decrease during cycling, which are similar technical hurdles found in Li–S battery, to realize the high performance Na/S battery. Although a cheap and flexible battery can contributes to commercialization of a lot of flexible electronic devices, there was no study into the possibility of flexible Na/S cells operating at room temperature [13].

Since most active materials are rigid, previous studies have tended to focus on combining them with flexible current collectors (or conducting agents) made from carbon materials or conductive paper, polymer, etc. [8,18]. This has meant that the preparation methods usually consist of two steps: the preparation of a flexible current collector, followed by its combination with a rigid active material [8]. Various methods have been used for this, such as hydrothermal reaction [19], photothermal reduction [20], pulsed laser deposition [21], ultrasonication and co-deposition [22], casting and drying [23].

Unfortunately, all of these methods bear fundamental and inevitable limitations. The foremost among these is the need for a flexible current collector that has both good flexibility and high electrical conductivity. Secondly, the flexible current collector reduces the capacity of the electrode due to its weight. Another limitation is the detachment of the active materials from the current collector by a severe physical deformation or the electrochemical reactions. Furthermore, a secondary step to attach the active material requires complex process and additional cost. Therefore, there is a strong need for a new approach to the flexible cathode which consists of only active material without a separate current collector. This concept offers many advantages in terms of simplifying the preparation process, eliminating the detachment of active material, and, most importantly, increasing the total electrode capacity. The realization of a single-body flexible cathode has, however, been delayed by the difficulties associated with achieving the right combination of high flexibility, good electrical conductivity, and good electrochemical reactivity.

Sulfurized polyacrylonitrile is well known as a cheap and high capacity cathode material suitable for lithium and sodium rechargeable cells [24–26]. During heat treatment,

polyacrylonitrile forms a heterocyclic ring that provides a high electrical conductivity of 10<sup>-4</sup> S cm<sup>-1</sup> [26]. Thus it can be possibly used as an electrode without current collector. In addition the electrochemical properties can be further improved by varying its morphology to nanonets or nanofibers [27,28].

It is well known that a rigid material can be flexible without fracture when it has a specific nanometer scale structure: Carbon can be flexible in the forms of carbon nanotube and nanofiber [29]. Thus, in this study, SPAN webs were fabricated through the simple heat treatment with the sulfur of electrospun PAN nanofiber webs. This experiment aimed at producing a flexible cathode without a binder, conducting agent, and current collector. The electrochemical properties of the flexible SPAN cathode vs Na/Na<sup>+</sup> are investigated. In addition, the charge/discharge mechanism is clarified using a singular cathode.

## 2. Experimental

### 2.1. Preparation of SPAN webs

The SPAN webs were prepared by a two-step process of electrospinning PAN nanofiber webs and their pyrolysis with sulfur. An electrospinning solution was prepared by dissolving PAN (10 wt%, Mw = 150,000, Polyscience, USA) in *N,N*-dimethylformamide (DMF, DAEJUNG, Korea) and homogeneously dispersing it by stirring at 60 °C for 12 h. This solution (4 mL) was then loaded into a 10 mL syringe fitted with a 21-gauge metallic needle (ID: 0.51 mm, OD: 0.81 mm) at its end. A flow rate of 1.8 mL h<sup>-1</sup> and high voltage of 19 kV was then applied to the needle, with the PAN nanofibers being then collected on a rotating drum (180 rpm) positioned about 18 cm from the needle tip. The as-spun PAN nanofiber web (PAN web) was then removed from the drum collector and set in an alumina boat. Afterward it was homogeneously covered with sulfur powder (Aldrich). The alumina boat was then transferred into a quartz tube furnace and pyrolyzed at 450 °C for 6 h at a heating rate of 10 °C min<sup>-1</sup> under an Ar atmosphere (100 sccm flow rate). Following this, the SPAN web was analyzed by a micro element analyzer (Flash 2000 CHNS/O Analyzer, Thermo scientific, USA) (see Supporting Information, Table S1), and then punched to form a 1 cm-diameter disc that was used directly as a cathode and has a weight from 0.73 mg with a thickness of ca. 30 μm. For comparative purposes, a HT-PAN web was also obtained by pyrolyzing the PAN web under the same conditions, but without the addition of sulfur.

### 2.2. Electrochemical characterization

A sodium metal disc (Aldrich, 99%) and 1 M of NaPF<sub>6</sub> in ethylene carbonate (EC) and diethyl carbonate (DEC) (1:1 = v/v, Soulbrain, Korea) were used as the anode and the electrolyte, respectively. A glass fiber filter (GF/D, Whatman, UK) was used as a separator. A SPAN web was used as a cathode without conducting agent, binder and current collector. Assembly of the Na/SPAN cell was carried out by sequentially stacking the sodium anode, glass fiber filter separator, and SPAN web. Swagelok-type cell containers were used for this, and all stages of assembly were conducted in an argon-filled glove box.

Electrochemical characterization was performed through galvanostatic tests carried out at room temperature using a WBCS3000 battery cyler (WonATech Co., Korea). A voltage range between 0.7 and 2.8 V vs. Na/Na<sup>+</sup> was selected, and the current densities of 0.01, 0.1, 0.5 and 1 C rates were selected based on the sulfur content of the SPAN web samples. Potentiostatic testing was conducted by means of a frequency response analyzer (VMP3, Biologic, France) operating at a scan rate of 0.1 mV s<sup>-1</sup> and at room temperature.

### 2.3. Characterization

In order to assess any change in the surface morphology during charge and discharge, the Na/SPAN cells were first disassembled in an argon-filled glove box and the SPAN web was rinsed in diethyl carbonate (DEC, Soulbrain, Korea) for more than 5 min. This was then dried in the same argon-filled glove box without exposure to air at room temperature for more than 3 days. The dried SPAN webs were subsequently transferred to a field-emission scanning electron microscope (FESEM, Quanta3D, FEI, Netherlands) without exposure to air by means of an argon-filled transfer chamber. Energy-dispersive X-ray spectroscopy (EDS, SiriusSD, e2v, UK) was also used for elemental mapping.

Detailed characterization of the various chemical bonds in each sample was performed using a HR Micro Raman spectrometer (LabRAM HR800 UV, Horiba Jobin Yvon, France) equipped with a 514 nm argon-ion laser. For this, the SPAN webs were sealed in a specially designed holder under an argon atmosphere to prevent their contamination by air.

Characterization by a 300 kV field emission transmission electron microscope (HR-TEM; 300 kV, TF30ST, Technai, USA) was coupled with energy-dispersive X-ray spectroscopy (EDS, QuantaX, Bruker, Germany) to analyze the SPAN web samples. During the transfer of these samples from the argon-filled glove box to the HR-TEM, they were exposed to the air for less than 1 min.

### 3. Results and discussion

Fig. 1 (a) shows photographs of an as-electrospun PAN web (PAN web), the PAN web after heat treatment (HT-PAN web) and a SPAN web before and after bending to 180°. In its as-spun state, the PAN web was highly flexible and able to be bended like a sheet of paper. Furthermore, it showed no discernible recovery from the bended state (see Supporting Information, movie clips). The HT-PAN web, on the other hand, was so rigid and brittle that it fractured when bent. More significantly, the SPAN web exhibited very different physical properties, being even more like paper than the as-spun PAN web. This gave it a very high flexibility, rollability, and bendability to 180° and it easily recovered its original shape. These results indicate that the SPAN web is very suitable for use as a cathode in a flexible cell.

Supplementary data related to this article can be found online at <http://dx.doi.org/10.1016/j.jpowsour.2015.12.035>.

The bendable SPAN web shown in Fig. 1 (a) was used directly (i.e. without a binder, current collector and additional conductive material) as a cathode in conjunction with a metallic Na. Fig. 1 (b) presents the cyclic voltammetry curves obtained over two initial cycles at a scan rate of 0.1 mV s<sup>-1</sup>. A large cathodic peak appeared at 0.85 V during the first reduction reaction. This peak became smaller and shifted to a higher voltage of 1.16 V in the following scan, with one small peak also appearing at 1.61 V. A broad peak at 1.62 V evident during the first oxidation reaction, however, was slightly shifted to 1.78 V without a change in shape during the second

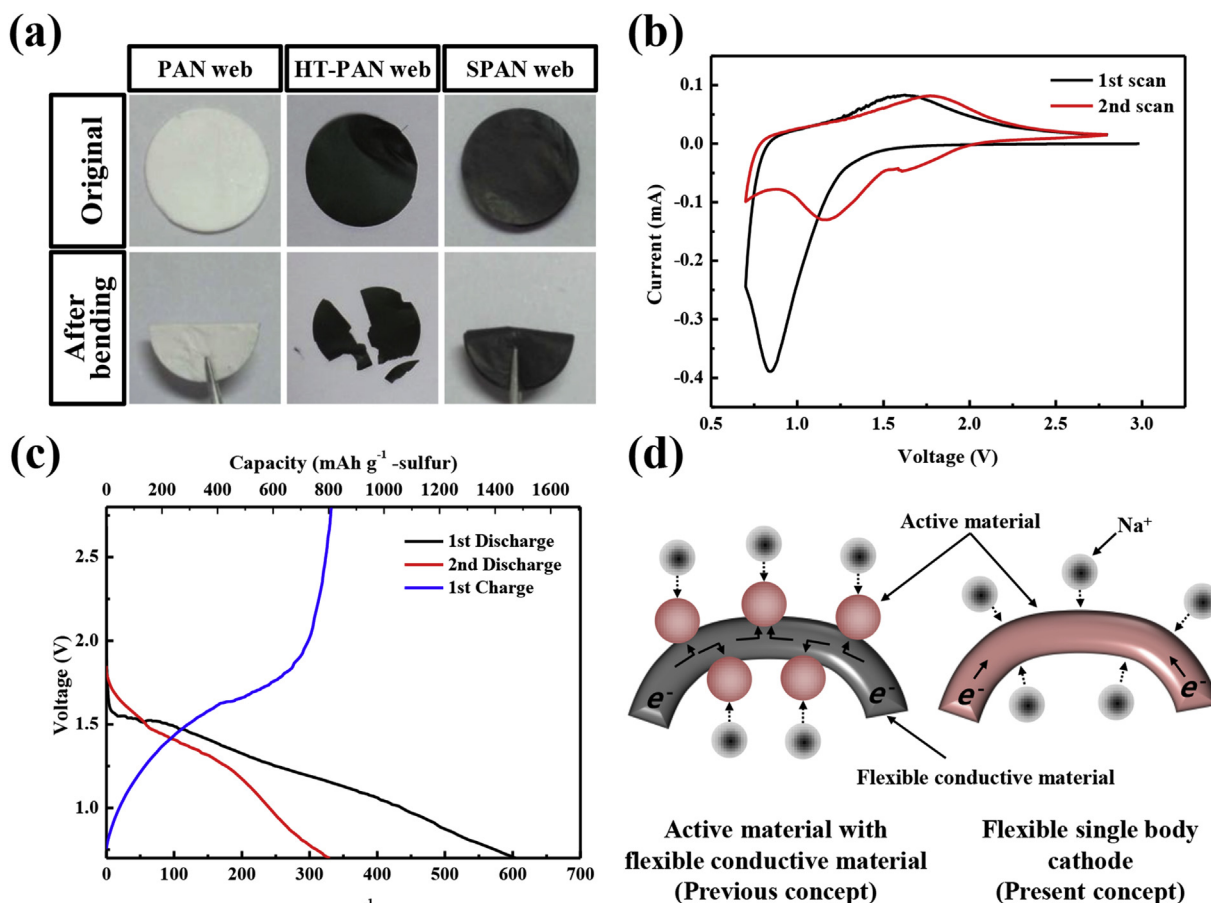


Fig. 1. (a) PAN web, HT-PAN web, and SPAN web before and after bending to 180°, (b) cyclic voltammetry, (c) charge/discharge curves to the second discharge of the SPAN web, and (d) schematic showing the previously reported concept (left) and the present concept (right) for flexible cathode.

oxidation reaction. These results imply that the SPAN web can function alone as a cathode, despite the absence of an additional conducting agent.

A Na/SPAN cell was charged and discharged at a rate of 0.01 C based on this sulfur content. The resulting charge and discharge curves in Fig. 1 (c) show that the first discharge capacity reached  $604 \text{ mAh g}^{-1}$  – electrode. Since the SPAN web contained 41 wt% sulfur (see Supporting Information, Table S1), the  $604 \text{ mAh g}^{-1}$  – electrode is corresponding to  $1473 \text{ mAh g}^{-1}$  – sulfur, i.e., 1.76 sodium per one sulfur. And the first discharge curve showed a plateau at 1.5 V that was followed by a gradual decline. During the first charge, a capacity of  $332 \text{ mAh g}^{-1}$  – electrode ( $810 \text{ mAh g}^{-1}$  – sulfur) was obtained and the first charge curve exhibiting a single sloping plateau at around 1.7 V. The Na/SPAN cell showed no plateau at the second discharge, which is well known for SPAN from the previous results [24,28], while the Na/S battery with elemental sulfur cathode shows two plateaus at  $\sim 2.2$  and 1.7 V, respectively, by reducing  $\text{S}_8$  (elemental sulfur) to  $\text{Na}_2\text{S}$ . This can imply that only 1 sodium ion per a sulfur atom returned to the sodium anode. During the next second discharge, the capacity of  $329 \text{ mAh g}^{-1}$  – electrode ( $802 \text{ mAh g}^{-1}$  – sulfur) was delivered giving an irreversible capacity loss of  $275 \text{ mAh g}^{-1}$  – electrode compared to the first discharge capacity. Unlikely to the first discharge curve, the second curve started at a higher voltage that then continuously declined. This can be attributed to the fact that the second cathodic peak is very small and close to the first one as shown in Fig. 1 (b).

Fig. 1 (d) shows a schematically rendered concept of the present flexible cathode in comparison with a previously reported examples [8], in which the active material is confined within a flexible current collector. This reveals several inherent drawbacks: Complex preparation process, physical detachment of active material from the flexible current collector by mechanical deformation and a reduction in capacity due to the use of electrochemically inert substrates. In contrast, the SPAN web cathode consists of only a single flexible material which is fabricated by a simple pyrolysis process and, thus, is free from the above drawbacks. And the results in Fig. 1 (b) and c clearly demonstrate that electrons move through the SPAN and the SPAN web works well as the flexible cathode.

Since the cathode is composed of only active material without binder, conducting agent and current collector, it is easy to clarify the electrochemical mechanism during charge/discharge. To understand their electrochemical behaviors, the SPAN webs were collected after discharge and charge. Fig. 2 (a) presents FESEM images obtained from these SPAN webs, in which they consist of straight SPAN nanofibers. The SPAN nanofibers have diameters of several hundred nanometers with high aspect ratio, which might be the origin of the flexibility. To our knowledge this is the first report for a fully flexible cathode with only an active material. This morphology was maintained after the second discharge, and as shown in Fig. 2 (a), there was no evidence of any new foreign particles or defects such as cracks, cleavages, and dents on the SPAN nanofibers. This means that the SPAN web itself remains stable during the electrochemical reactions.

The changes of the chemical composition during charge/discharge were analyzed by EDS as shown in Fig. 2 (b). Sodium plays a key role in the overall electrochemical reaction, as it is strongly believed to react with sulfur. The sodium to sulfur ratio is summarized at the upper part in Fig. 2 (b). After the first discharge there were 1.71 sodium atoms per sulfur atom, but this ratio decreased to 0.83 during the first charge. Afterward it returned to 1.9 during the next discharge. The first discharge capacity in Fig. 1 (c) is well matched with the ratio of sodium to sulfur in Fig. 2 (b). Thus the capacity should come from the electrochemical reaction of sodium to sulfur without side reactions. Some of sodium remains in SPAN web after first charge, which should be the origin of small

capacity of first charge and second discharge in Fig. 1 (c). Thus the irreversibility at second discharge can be explained by the stable sodium of SPAN web. Also, 1 sodium atom per sulfur atom reversibly participates in the electrochemical reactions, which is well matched with second discharge capacity in Fig. 1 (c). The elemental composition of SPAN web is shown at the lower part in Fig. 2 (b). Also, it was found that the atomic ratio of C:S:N in the original SPAN web was ca. 3:1:1, and is similar to the results of previous studies [25,28]. The same ratio was preserved after charge and discharge, which suggests that the molecular structure of the SPAN web was maintained and that sulfur did not dissolve into the electrolyte during electrochemical reactions.

The four samples in Fig. 2 (a) were further characterized by Raman spectroscopy to verify the existence of C–S bonds in the SPAN material and their changes during electrochemical reaction. As shown in Fig. 2 (c), the original SPAN web produced peaks at 314, 371, 394, 480, 920, 1300, and  $1500 \text{ cm}^{-1}$ . The latter two are generally assigned to the disordered (D mode) and graphite like (G-band) structures of carbon, respectively [28]. These two peaks were also observed with the HT-PAN web (see Fig. S1). The first five peaks below  $1000 \text{ cm}^{-1}$  were attributed to the reaction of PAN with sulfur (see Fig. S1). However, the patterns are different from previous results, which might be related to single SPAN without binder and conducting additives [25,28,30]. The peaks at 314, and  $371 \text{ cm}^{-1}$  were assigned to C–S bonds, and the peaks at 480 and  $920 \text{ cm}^{-1}$  to S–S bonds, but  $394 \text{ cm}^{-1}$  is not clear yet [30]. The C–S bond might come from sulfur bonded with carbon of heterocyclic ring, which is believed due to sulfur which covalently bonds to the PAN backbone in the chain structure [31] and might result in the sloping discharge curve in Fig. 1 (c). Furthermore, all of the five peaks below  $1000 \text{ cm}^{-1}$  exhibited electrochemical reversibility, disappearing after first and second discharge and reappearing after first charge. These results clearly prove that the C–S and S–S bonds are broken and reversibly reconnected during discharge and charge, respectively. This is a clear evidence for the electrochemical reversibility of C–S and S–S bonds in the SPAN. As demonstrated in the Raman results and elemental analyses, sulfur chemically bonds to the PAN backbone, which means that sulfur exists within the PAN nanofiber uniformly. If sodium reacts with sulfur, then the sodium must be matched with sulfur, in carbon matrix.

Fig. 2 (d) represents the changes of HR-TEM images, selected area electron diffraction (SAED) pattern, and EDS results of SPAN nanofiber by charge and discharge. Original SPAN nanofiber showed a blurred ring SAED pattern indicative of an amorphous structure and a similar pattern was obtained in the case of charge or discharge. From the EDS and Raman results, it is clear that there was a uniform distribution of sulfur and sodium within the SPAN nanofibers of all the SPAN webs, which means that the amorphous discharge products are generated uniformly and repeatedly within the SPAN nanofibers without partial agglomeration during electrochemical reaction. The SPAN nanofibers also showed clear signs of the presence of sodium after the first charge, which is consistent with the results in Fig. 2 (b).

Prior to the cycle performance testing, the SPAN web cathode was pre-cycled once at 0.01 C (see Fig. S2). Fig. 3 (a) shows the typical charge and discharge curves that were subsequently obtained for the first, second, 20th, and 200<sup>th</sup> cycle at a rate of 0.1 C. Note that the first discharge curve has no clear plateau, but instead shows a continuous voltage decline; a tendency that was maintained in the other discharge curves with a high reversibility. Fig. 3 (b) presents the cycling behavior of the SPAN web cathode. The first discharge capacity of  $342 \text{ mAh g}^{-1}$  – electrode was obtained. From the second cycle, a stable discharge capacity of  $257 \text{ mAh g}^{-1}$  – electrode was delivered and maintained during 200 cycles along with a capacity of  $266 \text{ mAh g}^{-1}$  – electrode. The coulombic

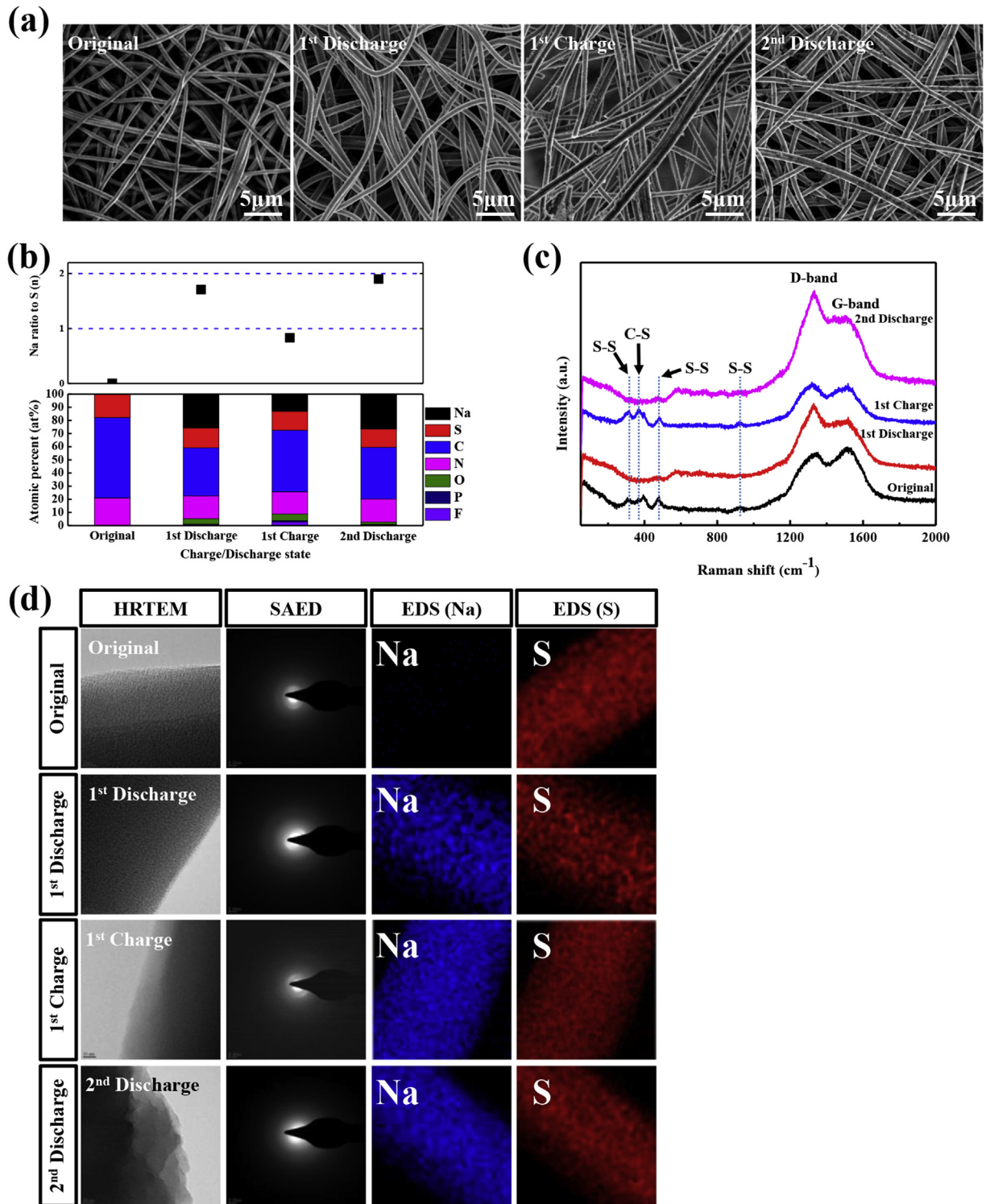


**Fig. 2.** (a) FESEM micro images, (b) atomic ratio of sodium to sulfur and elemental composition (EDS results), (c) Raman spectra, and (d) HR-TEM analyses of the SPAN web after each charge and discharge.

efficiency was near 100% from the second cycle. Since SPAN web cathode did not contain binder, conducting agent and current collector, the capacity of 266 mAh g<sup>-1</sup> – electrode after 200 cycles is higher than flexible cathode for lithium ion batteries [32–37]. Fig. 3 (c) shows the rate capability from 0.01 C to 1C relative to the sulfur loading, which reveals that the SPAN web cathode is capable of delivering ca. 310 mAh g<sup>-1</sup> – electrode at 0.01 C. An increase in the

discharge rate causes the capacity to gradually decrease, but it still remains as high as 72 mAh g<sup>-1</sup> – electrode at 1C. In spite of the lack of any additional conducting material, the high porosity, high surface area should have contributed to this excellent rate capability.

Investigation of the SPAN web cathode after cycling by FESEM confirmed that it retained its original morphology without any deterioration such as cracks, cleavages, and dents on the SPAN

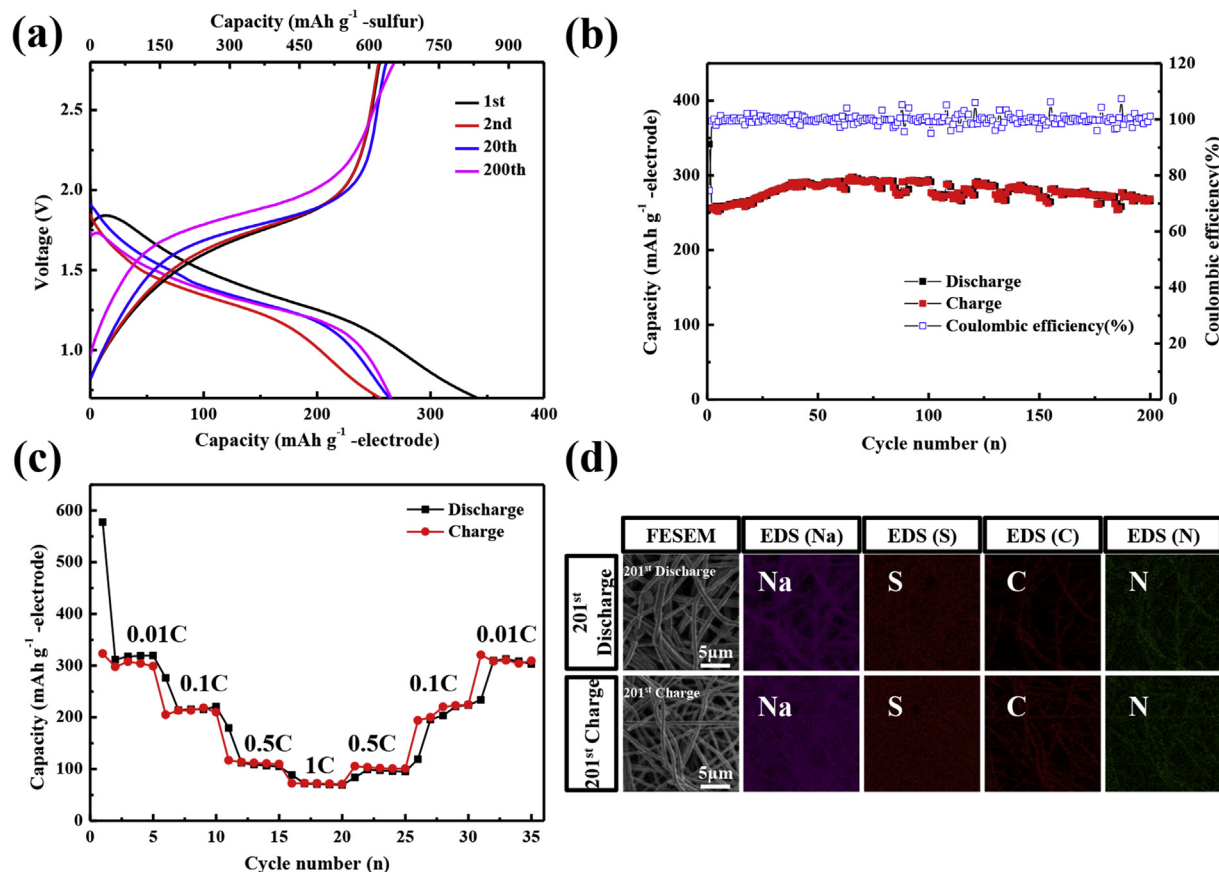


Fig. 3. (a) Typical charge/discharge curves, (b) cycle performance over 200 cycles at 0.1 C, (c) rate capability from 0.01 to 1 C, and (d) EDS analyses of the SPAN web after 200 cycles.

nanofibers after 200 cycles. The distribution of Na in the SPAN web was in a good accordance with the FESEM images and EDS results of C and N elements. These indicate that the SPAN web well maintained its morphology during repeated cycling. The good cycling property is likely owing to the reliable structure of the SPAN web cathode.

Commercial carbon fiber is easily produced by heating PAN fiber. Thus, the SPAN web can be prepared using same facilities because SPAN can be prepared through heating the PAN fiber with sulfur. Especially, S, PAN and Na are abundant and cheap materials. This presents a huge potential to commercialize the flexible and low cost Na/S cells. Further, this concept can be applicable to the Li/S battery.

#### 4. Conclusions

This study has demonstrated that a flexible web cathode produced solely from SPAN offers high flexibility, rollability, and bendability to 180° without any fracture. The reversible electrochemical reaction of this SPAN web with sodium was proven to be the result of reversible cleavage/bond formation between the C–S and S–S bonds of the SPAN web. During the charge/discharge test at 0.01 C based on sulfur content, the SPAN web delivered a high first discharge capacity of 604  $\text{mAh g}^{-1}$  – electrode (1473  $\text{mAh g}^{-1}$  – sulfur). It also produced a good cycling performance over 200 cycles, as well as a high capacity of 266  $\text{mAh g}^{-1}$  – electrode after the 200<sup>th</sup> cycle. In rate measurements, it delivered a capacity as high as 71  $\text{mAh g}^{-1}$  – electrode at 1C. Since PAN fiber is an inexpensive material produced in commercial quantities for the manufacture of carbon fibers, its modification to SPAN through

pyrolysis with sulfur requires only minimal additional facilities. This presents a huge potential to the commercialization of the SPAN web material, making it a very promising candidate for the realization of low cost and flexible Na/S cells.

#### Acknowledgment

This work was supported by the National Research Foundation of Korea (NRF) grant funded by the Korea government (MEST) (No. 2013R1A2A1A01015911).

#### Appendix A. Supplementary data

Supplementary data related to this article can be found at <http://dx.doi.org/10.1016/j.jpowsour.2015.12.035>.

#### References

- [1] D.-H. Kim, Y.-S. Kim, J. Wu, Z. Liu, J. Song, H.-S. Kim, Y.Y. Huang, K.-C. Hwang, J.A. Rogers, *Adv. Mater.* 21 (2009) 3703–3707.
- [2] B.D. Gates, *Science* 323 (2009) 1566–1567.
- [3] C. Pang, C. Lee, K.-Y. Suh, *J. Appl. Polym. Sci.* 130 (2013) 1429–1441.
- [4] M.L. Hammock, A. Chortos, B.C. Tee, J.B. Tok, Z. Bao, *Adv. Mater.* 25 (2013) 5997–6038.
- [5] W. Zeng, L. Shu, Q. Li, S. Chen, F. Wang, X.M. Tao, *Adv. Mater.* 26 (2014) 5310–5336.
- [6] B.Y. Ahn, E.B. Duoss, M.J. Motala, X. Guo, S.I. Park, Y. Xiong, J. Yoon, R.G. Nuzzo, J.A. Rogers, J.A. Lewis, *Science* 323 (2009) 1590–1593.
- [7] G. Park, H.J. Chung, K. Kim, S.A. Lim, J. Kim, Y.S. Kim, Y. Liu, W.H. Yeo, R.H. Kim, S.S. Kim, J.S. Kim, Y.H. Jung, T.I. Kim, C. Yee, J.A. Rogers, K.M. Lee, *Adv. Healthc. Mater.* 3 (2014) 515–525.
- [8] G. Zhou, F. Li, H.-M. Cheng, *Energy Environ. Sci.* 7 (2014) 1307–1338.
- [9] C.-W. Park, J.-H. Ahn, H.-S. Ryu, K.-W. Kim, H.-J. Ahn, *Electrochem. Solid-State Lett.* 9 (2006) A123.

- [10] J.-S. Kim, H.-J. Ahn, I.-P. Kim, K.-W. Kim, J.-H. Ahn, C.-W. Park, H.-S. Ryu, J. Solid State Electrochem. 12 (2008) 861–865.
- [11] D. Kumar, M. Suleman, S.A. Hashmi, Solid State Ion. 202 (2011) 45–53.
- [12] H. Ryu, T. Kim, K. Kim, J.-H. Ahn, T. Nam, G. Wang, H.-J. Ahn, J. Power Sources 196 (2011) 5186–5190.
- [13] S. Wenzel, H. Metelmann, C. Raiß, A.K. Dürr, J. Janek, P. Adelhelm, J. Power Sources 243 (2013) 758–765.
- [14] I. Bauer, M. Kohl, H. Althues, S. Kaskel, Chem. Commun. 50 (2014) 3208–3210.
- [15] S. Xin, Y.-X. Yin, Y.-G. Guo, L.-J. Wan, Adv. Mater. (2013) 1261–1265.
- [16] X. Yu, A. Manthiram, Adv. Energy Mater. (2015), 1500350.
- [17] I. Kim, J.-Y. Park, C.H. Kim, J.-W. Park, J.-P. Ahn, J.-H. Ahn, K.-W. Kim, H.-J. Ahn, J. Power Sources 301 (2016) 332–337.
- [18] M.-S. Jung, J.-H. Seo, M.-W. Moon, J.W. Choi, Y.-C. Joo, I.-S. Choi, Adv. Energy Mater. 5 (2015) 1400611.
- [19] X. Jia, Z. Chen, A. Suwarnasarn, L. Rice, X. Wang, H. Sohn, Q. Zhang, B.M. Wu, F. Wei, Y. Lu, Energy Environ. Sci. 5 (2012) 6845.
- [20] X. Zhao, C.M. Hayner, M.C. Kung, H.H. Kung, Chem. Commun. 48 (2012) 9909–9911.
- [21] H. Gwon, H.-S. Kim, K.U. Lee, D.-H. Seo, Y.C. Park, Y.-S. Lee, B.T. Ahn, K. Kang, Energy Environ. Sci. 4 (2011) 1277.
- [22] S. Luo, K. Wang, J. Wang, K. Jiang, Q. Li, S. Fan, Adv. Mater. 24 (2012) 2294–2298.
- [23] L. Jabbour, C. Gerbaldi, D. Chaussy, E. Zeno, S. Bodoardo, D. Beneventi, J. Mater. Chem. 20 (2010) 7344.
- [24] J. Wang, J. Yang, Y. Nuli, R. Holze, Electrochem. Commun. 9 (2007) 31–34.
- [25] J. Wang, J. Yang, C. Wan, K. Du, J. Xie, N. Xu, Adv. Funct. Mater. 13 (2003) 487–492.
- [26] J. Wang, Y.S. He, J. Yang, Adv. Mater. 27 (2015) 569–575.
- [27] Y. Zhang, Y. Zhao, Z. Bakenov, A. Konarov, P. Chen, J. Power Sources 270 (2014) 326–331.
- [28] T.H. Hwang, D.S. Jung, J.-S. Kim, B.G. Kim, J.W. Choi, Nano Lett. 13 (2013) 4532–4538.
- [29] G. Cao, Nanostructures & Nanomaterials: Synthesis, Properties & Applications, Imperial College Press, London UK, 2004.
- [30] X.-g. Yu, J.-y. Xie, J. Yang, H.-j. Huang, K. Wang, Z.-s. Wen, J. Electroanal. Chem. 573 (2004) 121–128.
- [31] J. Fanous, M. Wegner, J. Grimming, Ä. Andresen, M.R. Buchmeiser, Chem. Mater. 23 (2011) 5024–5028.
- [32] J.-Z. Wang, S.-L. Chou, J. Chen, S.-Y. Chew, G.-X. Wang, K. Konstantinov, J. Wu, S.-X. Dou, H.K. Liu, Electrochem. Commun. 10 (2008) 1781–1784.
- [33] L. Jabbour, M. Destro, D. Chaussy, C. Gerbaldi, N. Penazzi, S. Bodoardo, D. Beneventi, Cellulose 20 (2012) 571–582.
- [34] S. Leijonmarck, A. Cornell, G. Lindbergh, L. Wågberg, Nano Energy 2 (2013) 794–800.
- [35] S. Leijonmarck, A. Cornell, G. Lindbergh, L. Wågberg, J. Mater. Chem. A 1 (2013) 4671.
- [36] Y.H. Ding, H.M. Ren, Y.Y. Huang, F.H. Chang, P. Zhang, Mater. Res. Bull. 48 (2013) 3713–3716.
- [37] Q. Lu, G.S. Hutchings, Y. Zhou, H.L. Xin, H. Zheng, F. Jiao, J. Mater. Chem. A 2 (2014) 6368.